Isolation and characterization of tick-borne *Roseomonas haemaphysalidis* sp. nov. and rodent-borne *Roseomonas marmotae* sp. nov.[§]

Wentao Zhu[1], Juan Zhou[1], Shan Lu[1,2,3], Jing Yang[1,2,3], Xin-He Lai[4], Dong Jin[1,2,3], Ji Pu[1], Yuyuan Huang[1], Liyun Liu[1], Zhenjun Li[1], and Jianguo Xu[1,2,3*]

[1]*State Key Laboratory of Infectious Disease Prevention and Control, National Institute for Communicable Disease Control and Prevention, Chinese Center for Disease Control and Prevention, Changping, Beijing 102206, P. R. China*
[2]*Shanghai Public Health Clinical Center, Fudan University, Shanghai 201508, P. R. China*
[3]*Research Units of Discovery of Unknown Bacteria and Function, Chinese Academy of Medical Sciences, Beijing 100730, P. R. China*
[4]*Henan Key Laboratory of Biomolecular Recognition and Sensing, College of Chemistry and Chemical Engineering, Henan Joint International Research Laboratory of Chemo/Biosensing and Early Diagnosis of Major Diseases, Shangqiu Normal University, Shangqiu 476000, P. R. China*

Four novel Gram-negative, mesophilic, aerobic, motile, and cocci-shaped strains were isolated from tick samples (strains 546[T] and 573) and respiratory tracts of marmots (strains 1318[T] and 1311). The 16S rRNA gene sequencing revealed that strains 546[T] and 573 were 97.8% identical to *Roseomonas wenyumeiae* Z23[T], whereas strains 1311 and 1318[T] were 98.3% identical to *Roseomonas ludipueritiae* DSM 14915[T]. In addition, a 98.0% identity was observed between strains 546[T] and 1318[T]. Phylogenetic and phylogenomic analyses revealed that strains 546[T] and 573 clustered with *R. wenyumeiae* Z23[T], whereas strains 1311 and 1318[T] grouped with *R. ludipueritiae* DSM 14915[T]. The average nucleotide identity between our isolates and members of the genus *Roseomonas* was below 95%. The genomic G+C content of strains 546[T] and 1318[T] was 70.9% and 69.3%, respectively. Diphosphatidylglycerol (DPG) and phosphatidylethanolamine (PE) were the major polar lipids, with Q-10 as the predominant respiratory quinone. According to all genotypic, phenotypic, phylogenetic, and phylogenomic analyses, the four strains represent two novel species of the genus *Roseomonas*, for which the names *Roseomonas haemaphysalidis* sp. nov. and *Roseomonas marmotae* sp. nov. are proposed, with 546[T] (= GDMCC 1.1780[T] = JCM 34187[T]) and 1318[T] (= GDMCC 1.1781[T] = JCM 34188[T]) as type strains, respectively.

Keywords: *Roseomonas haemaphysalidis*, *Roseomonas marmotae*, tick, marmot, Qinghai-Tibet plateau

*For correspondence. E-mail: xujianguo@icdc.cn
§Supplemental material for this article may be found at http://www.springerlink.com/content/120956.

Introduction

The genus *Roseomonas*, belonging to the family *Acetobacteraceae* within the order *Rhodospirillales*, was originally proposed in 1993 (Rihs *et al.*, 1993), and emended in 2010 (Venkata Ramana *et al.*, 2010). The cells of *Roseomonas* are non-spore forming, mesophilic, Gram-negative, cocci or coccoid-shaped, and non-motile (Kim *et al.*, 2013), with pink, circular, pulvinate, and smooth colonies (Tian *et al.*, 2019). As of April 2021, the genus comprises 45 validly published and correctly named species (https://lpsn.dsmz.de/genus/roseomonas). Their primary cellular fatty acid is $C_{18:1}\omega 7c/C_{18:1}\omega 6c$, with diphosphatidylglycerol and phosphatidylethanolamine as dominant polar lipids and Q-10 as the major isoprenoid quinone (Sánchez-Porro *et al.*, 2009; Kim *et al.*, 2013; Tian *et al.*, 2019). The genomic DNA G + C content of species in the genus *Roseomonas* ranges from 68.6 to 73.0% (Sánchez-Porro *et al.*, 2009; Kim *et al.*, 2013; Tian *et al.*, 2019; Li *et al.*, 2021).

Although the majority of species of genus *Roseomonas* are non-pathogenic and have been isolated from several environmental sources, such as air, marine, invertebrates, soil, water, copper alloy coins, skin, and plants (Shao *et al.*, 2019), certain members are known to cause opportunistic infections in humans. For example, *R. mucosa*, although with low pathogenicity to healthy humans and occasionally isolation from clinical specimens, is an opportunistic pathogen, especially to immunocompromised individuals, causing spondylodiskitis, skin and soft tissue infections, septic arthritis, and bacteremia. In contrast, compared to other members of the genus, *R. gilardii* has been commonly isolated from patients with leukemia and acute appendicitis (Mulita *et al.*, 2020). Although rarely reported for unknown reasons (Dé *et al.*, 2004), *Roseomonas* infection can be difficult to treat due to a high resistance rate (> 90%) to β-lactams (penicillin and piperacillin/tazobactam) (Ioannou *et al.*, 2020).

Ticks are parasitic arachnids that belong to the superorder *Parasitiformes* and are widely distributed globally, particularly in regions with warm and humid climates. Ticks feed on the blood of mammals, birds, and occasionally reptiles and amphibians (Guerrero *et al.*, 2012). Previously, intracellular pathogens such as *Anaplasmosis*, *Ehrlichia*, and *Rickettsia* have been isolated from ticks (Dantas-Torres *et al.*, 2012), with less focus on extracellular microorganisms. The Himalayan marmots, living in the Himalayas and the Qinghai-Tibet plateau at altitudes of 3,000 to 5,500 meters, are the reservoir of *Yersinia pestis* and coronavirus (Zhu *et al.*, 2021).

During our investigation on the microbial diversity of ticks

and marmots, four strains (546[T], 573, 1311, and 1318[T]) belonging to the genus *Roseomonas* were isolated. The strain 546[T] produces carotenoid, an important compound for the biotechnological and pharmaceutical industry (Yokoyama *et al.*, 1996; Booth *et al.*, 2017). Our polyphasic approach based on phenotypic, phylogenetic, phylogenomic, and chemotaxonomic data revealed that the four strains are different from currently recognized species and could represent two novel species within the genus *Roseomonas*, for which the names *Roseomonas haemaphysalidis* sp. nov. and *Roseomonas marmotae* sp. nov. are proposed.

Materials and Methods

Isolation and identification

Ticks and marmots were sampled, respectively, from Qinghai Province in 2018 and Jiangxi Province in 2019 and transferred to our laboratory in Beijing. Ticks were washed thrice in 75% ethanol, once in phosphate-buffered saline (PBS, pH 7.4), and ground in brain heart infusion (BHI) broth with Tissue Lyser II (Qiagen); the respiratory tracts of marmots were similarly treated. Next, about 100 μl of serially diluted homogenates was spread onto BHI plates with 5% sterile defibered sheep blood. After 3 days, colonies were selected and purified, and subsequently conserved at -80°C in BHI with 20% (v/v) glycerol for further identification. Based on 16S rRNA sequence similarities, *R. wenyumeiae* Z23[T], *R. ludipueritiae* DSM 14915[T], and *R. aerophila* NBRC 108923[T] were selected for parallel comparison.

Morphological, physiological, and biochemical characteristics

R2A broth was used to determine the optimum growth by monitoring OD_{600} changes in our strains after inoculation. Growth at eight temperatures (4, 12, 20, 28, 35, 40, 45, and 50°C), eight NaCl concentrations (0.5–7.5%, 1% intervals), and eight pH values (4–11, 1 intervals) was tested, respectively. Morphological and biochemical characteristics were subsequently examined under optimum conditions in R2A broth. Gram-staining was conducted using a Gram-staining kit as described in a previous report (Zhu *et al.*, 2020). Spore formation was studied using a nutrient sporulation medium (Lee *et al.*, 2013). Anaerobic growth was tested under both air plus 5% CO_2 and in an anaerobic incubator. The oxidase activity and catalase activity were evaluated using 0.1% (w/v) tetramethyl-p-phenylenediamine and 3% (v/v) H_2O_2 solution for bubble production (Liu *et al.*, 2020), respectively. The biomass cultured under optimum conditions in the R2A broth was used to examine the composition of fatty acids, isoprenoid quinones, and polar lipids. The polar lipids were identified using two-dimensional thin-layer chromatography (TLC) (Watanabe *et al.*, 1997; Oh *et al.*, 2020), and stained with ninhydrin (aminolipids), α-naphthol (glycolipids), Dittmer-Lester reagent (phospholipids), and molybdophosphoric acid (total polar lipids) (Kim *et al.*, 2021). The major fatty acids of the isolates and closely related type strains were extracted and analyzed according to the protocol described in a previous report (Athalye *et al.*, 1985; Zhu *et al.*, 2019). The isoprenoid quinones were examined as described previously (Collins and Jones, 1981). The polyamine pattern was detected using high-performance liquid chromatography (HPLC) as previously reported (Kim *et al.*, 2013). The isolates were biochemically tested using API 50CH, 20NE, and ZYM strips following the instructions.

Genome extraction and sequencing

Genomic DNA of our isolates was extracted using the Wizard Genomic DNA Purification Kit. The 16S rRNA genes were amplified using primers 27F and 1492R as previously reported (Frank *et al.*, 2008; Zhu *et al.*, 2020), cloned into the p*MD*18-T vector, and subjected to Sanger sequencing. The 16S rRNA gene sequences were searched using BLASTN in the rRNA databases of NCBI and EzBioCloud servers (Yoon *et al.*, 2017a). Afterward, the genomes of strains 546[T] and 1318[T] were sequenced by coupling the Pacific Biosciences sequel platform with Illumina short-read sequencing platform. The draft genomes of strains 573 and 1311 were sequenced on the Illumina platform. After filtering out the low-quality reads, the obtained clean data were *de novo* assembled using VELVET (Zerbino and Birney, 2008) and HGAP (Chin *et al.*, 2013) with default parameters.

Genomic analysis

The DNA-DNA relatedness was calculated and compared using Genome-to-Genome Distance Calculator 2.1 (http://ggdc.dsmz.de/) (Tao *et al.*, 2020). The average nucleotide identity (ANI) values were determined by FastANI (Jain *et al.*, 2018). The genomes were annotated by Rapid Annotation using Subsystem Technology (RAST) (Aziz *et al.*, 2008), and secondary metabolites were searched using antiSMASH (Blin *et al.*, 2019). The antimicrobial resistance gene family was predicted using the Comprehensive Antibiotic Resistance Database (Alcock *et al.*, 2020).

Phylogenetic and phylogenomic analyses

The 16S rRNA gene sequences of all strains concerned were aligned using the ClustalW algorithm and applied to phylogenetic analyses using MEGA version X with the neighbor-joining (NJ), maximum-likelihood (ML), maximum-parsimony (MP) algorithms (Kumar *et al.*, 2018), respectively. The protein sequences of core genes of genomes from genus *Roseomonas* were extracted using the CD-HIT software (Fu *et al.*, 2012) based on 0.4 protein sequence similarity and aligned to reconstruct a phylogenomic tree using FastTree (Price *et al.*, 2009).

Results and Discussion

Isolation and phenotypic characterization

The four novel strains were isolated from animals (ticks and marmots), similar to *R. wenyumeiae* Z23[T] (from Tibetan antelope). However, these were different from *R. aerophila* NBRC 108923[T] and *R. ludipueritiae* DSM 14915[T] of non-animal origin (Kämpfer *et al.*, 2003; Kim *et al.*, 2013). The cells were Gram-negative, non-spore forming, motile, and cocci-shaped with size ranging from 1.5 to 1.9 μm for strain 546[T],

Table 1. Differential biochemical properties that distinguish our isolates from the closely related type strains of the genus *Roseomonas*

Strains: 1, *Roseomonas haemaphysalidis* 546[T]; 2, *Roseomonas haemaphysalidis* 573; 3, *Roseomonas marmotae* 1311; 4, *Roseomonas marmotae* 1318[T]; 5, *R. wenyumeiae* Z23[T]; 6, *R. ludipueritiae* DSM 14915[T]; 7, *R. aerophila* NBRC 108923[T]. –, negative; +, positive; w, weak. All data are from this study.

Strains	1	2	3	4	5	6	7
Colony colour	Orange	Orange	White	White	Pink	Pink	White
Motility	+	+	+	+	+	–	+
Temperature range (°C)	4–45	4–45	4–35	4–35	20–37	20–45	4–40
API 50CH							
Glycerol	–	–	–	–	+	+	+
D-Glucose	–	–	–	–	+	+	+
D-Mannitol	–	–	–	–	+	+	+
D-Saccharose	–	–	–	–	–	–	+
L-Rhamnose	–	–	+	+	+	+	–
L-Xylose	–	–	+	+	+	+	+
Methyl β-D-xylopyranoside	–	–	+	+	+	+	+
API ZYM							
Esterase lipase (C8)	w	w	–	–	–	–	–
α-Glucosidase	+	+	–	–	–	–	+
API 20NE							
Nitrate reduction	–	–	+	+	–	–	–
Urease	+	+	–	–	+	+	+

and 1.7 to 2.1 µm for strain 1318[T] (Supplementary data Fig. S1), similar to the size of *R. wenyumeiae* Z23[T] but greater than that of *R. aerophila* NBRC 108923[T] and *R. ludipueritiae* DSM 14915[T] (Kämpfer *et al.*, 2003; Kim *et al.*, 2013). Colonies were circular, smooth, and orange (strains 546[T] and 573) or white (strains 1318[T] and 1311) after 3 days of growth on R2A plates. The four strains were catalase- and oxidase-positive. The growth was observable in the presence of 0.5 to 3.5% (w/v) NaCl (optimum, 0.5%) and at pH 6.0 to 9.0 (optimum, 8.0). The temperature ranges for growth were 4 to 45°C (optimum, 28°C) for strains 546[T] and 573, and 4 to 35°C (optimum, 28°C) for strains 1318[T] and 1311. All four strains could grow optimally under mesophilic conditions, and no growth was observed under anaerobic conditions. The orange colonies of strains 546[T] and 573 and white colonies of strains 1311 and 1318[T] (similar to *R. aerophila* NBRC 108923[T]) were distinct among all strains (Table 1). Our isolates were able to grow at 4°C, similar to *R. aerophila* NBRC 108923[T] but differed from *R. wenyumeiae* Z23[T] and *R. ludipueritiae* DSM 14915[T] (Table 1).

The biochemical characteristics indicated that strains 546[T] and 573 produced acids from D-arabinose, L-arabinose, D-fructose, D-fucose, L-fucose, D-lyxose, D-ribose, and D-xylose. Enzymatic activities of strains 546[T] and 573 were positive for esterase (C4), esterase lipase (C8), leucine arylamidase, and α-glucosidase. Strains 1318[T] and 1311 produced acids from D-arabinose, L-arabinose, D-fucose, and L-fucose, D-lyxose, D-melibiose, L-rhamnose, D-ribose, D-xylose, and L-xylose, but variable from D-fructose. Strains 1318[T] and 1311 were positive for esterase (C4) and leucine arylamidase activities. However, the four strains could not produce acid from glycerol, erythritol, D-adonitol, D-galactose, D-glucose, D-mannose, L-sorbose, dulcitol, inositol, D-mannitol, D-sorbitol, amygdalin, arbutin, esculin, D-maltose, D-lactose, glycogen, D-arabitol, or L-arabitol. In addition, the enzymatic activities of all four strains were negative for lipase (C14), valine arylamidase, cysteine arylamidase, trypsin arylamidase, α-

galactosidase, β-galactosidase, β-glucuronidase, β-glucosidase, α-fucosidase, or α-mannosidase. The summarized biochemical traits in Table 1 indicated that all four novel strains could not produce acid from glycerol, D-glucose, or D-mannitol, contrary to their three closest relatives. Strains 546[T] and 573 were weakly positive for esterase lipase (C8) but unable to produce acid from L-xylose or methyl β-D-xylopyranoside, opposite to all other strains across Table 1. Similarly, strains 1311 and 1318[T] were positive for nitrate reduction and negative for urease in marked contrast to all other strains (Table 1).

Phylogenetic analysis

A comparison against the EzTaxon-e database of new and almost-complete 16S rRNA gene sequences (all 1,452 bp) revealed that strains 546[T], 573, 1311, and 1318[T] were most closely related to the representatives of the genus *Roseomonas*. Strains 546[T] and 573 were closest to *R. wenyumeiae* Z23[T] (97.8% of 16S rRNA gene identity), whereas strains 1311 and 1318[T] were closest to *R. ludipueritiae* DSM 14915[T] (98.3%). The identity between strains 546[T] and 1318[T] was 98.0%. These values were lower than 98.7%, the generally accepted threshold for species (Rossi-Tamisier *et al.*, 2015), suggesting that the four isolates represented two novel species.

The 16S rRNA gene sequences of all type strains from the genus *Roseomonas* were aligned and subjected to phylogenetic analyses with NJ, ML, and MP algorithms, respectively. The treeing results (Fig. 1; Supplementary data Figs. S2 and S3) revealed that strains 546[T], 573, 1311, and 1318[T] belonged to the genus *Roseomonas*, forming independent clusters, respectively, with *R. wenyumeiae* Z23[T] and *R. ludipueritiae* DSM 14915[T] with high bootstrap values.

Genome characteristics

The sequencing results showed that each genome comprised one circular chromosome with either seven plasmids (strain
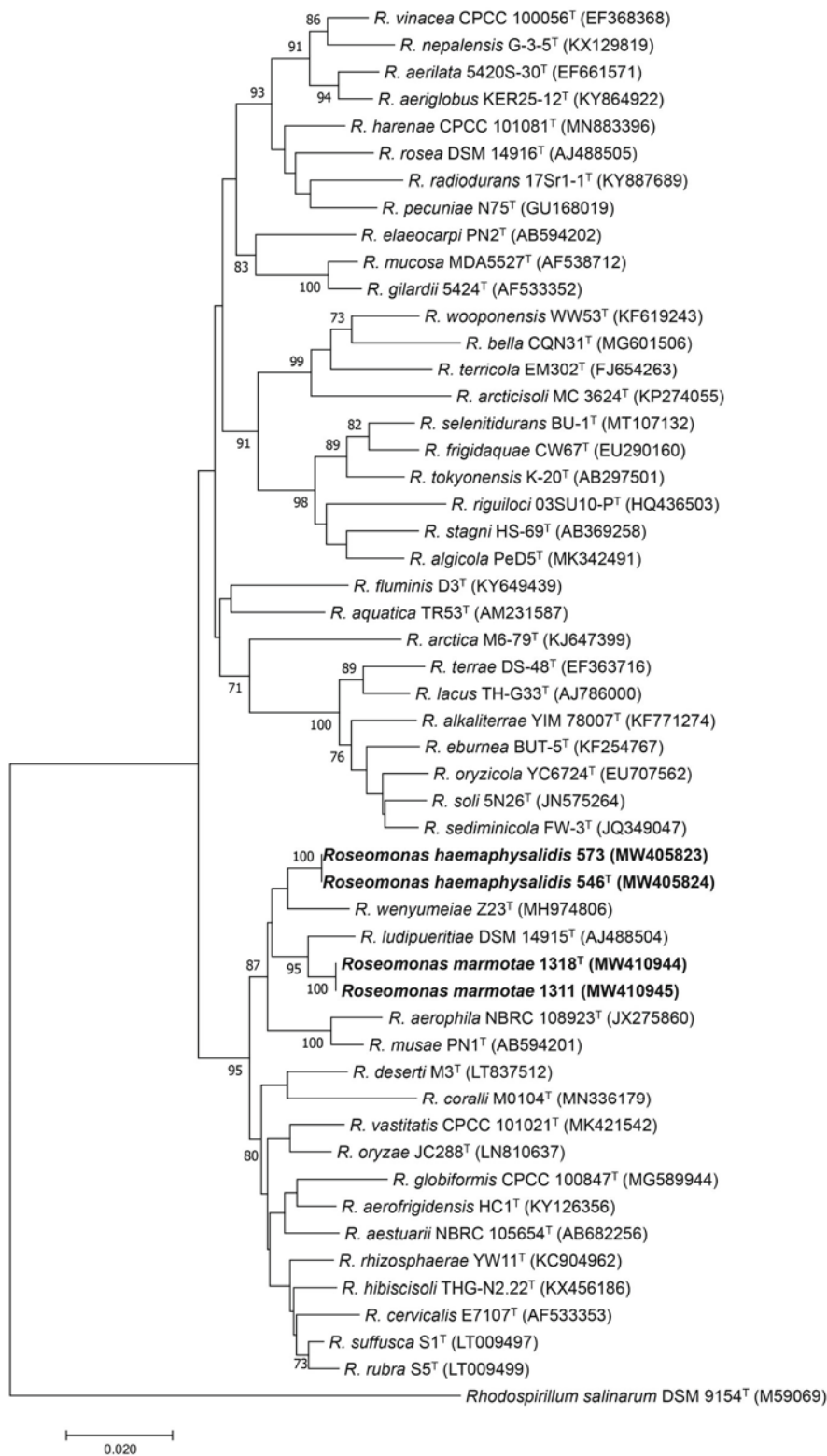
Fig. 1. Neighbor-joining phylogenetic tree based on nearly complete 16S rRNA gene sequences showing the relationships between our isolates and the type strains of the genus *Roseomonas.* Bootstrap values (70%) based on 1,000 replicates are shown at branch nodes, with *Rhodovibrio salinarum* DSM 9154[T] as an outgroup. Bar, 0.02 changes per nucleotide position. Strains from this study are highlighted in bold.

546[T]) or nine plasmids (strain 1318[T]). The draft genomes of strains 573 and 1311 were derived from 29 and 101 contigs, respectively. The genomic characteristics (G + C content, number of genes, size, etc.) compared with their closest relatives (Table 2) demonstrated that our isolates had smaller genomes (therefore fewer genes) and fewer pseudogenes, and strains 546[T] and 573 had a slightly higher G + C content than other compared strains.

Table 2. Genome features of strains 546^T, 573, 1311, 1318^T, and their closest relatives of genus *Roseomonas*
Strains: 1, *Roseomonas haemaphysalidis* 546^T; 2, *Roseomonas haemaphysalidis* 573; 3, *Roseomonas marmotae* 1311; 4, *Roseomonas marmotae* 1318^T; 5, *R. wenyumeiae* Z23^T; 6, *R. ludipueritiae* DSM 14915^T; 7, *R. aerophila* NBRC 108923^T. –, absence.

Characteristics	1	2	3	4	5	6	7
Size (Mb)	3.8	4.9	4.8	3.6	6.1	5.4	5.7
Contigs	1	29	104	1	196	394	140
Plasmids	7	–	–	9	–	–	–
N50 (bp)	3,777,460	287,631	190,323	3,565,232	179,822	26,901	86,979
Number of genes	3,533	4,581	4,535	3,379	5,747	5,297	5,095
Pseudogenes	44	39	72	92	151	211	140
G + C content (%)	70.9	70.3	68.9	69.3	68.6	68.8	68.9
rRNA	9	6	5	12	4	4	3
tRNA	50	48	47	52	48	44	45
Other RNA	4	4	4	4	6	4	4

The GenBank/EMBL/DDBJ accession numbers of plasmids for strains 546^T and 1318^T were CP061178-CP061184 and CP061092-CP061100, respectively.

Annotation of the complete genomes of strains 546^T and 1318^T on the RAST server exhibited that only 27% of genes were categorized into 25 subsystems for strain 546^T and 24 subsystems for strain 1318^T, whereas 73% of genes remained to be categorized into any subsystem (Supplementary data Fig. S4). Both genomes of strains 546^T and 1318^T contained four major subsystems for amino acids and derivatives, protein metabolism, carbohydrates, and cofactors/vitamins/prosthetic
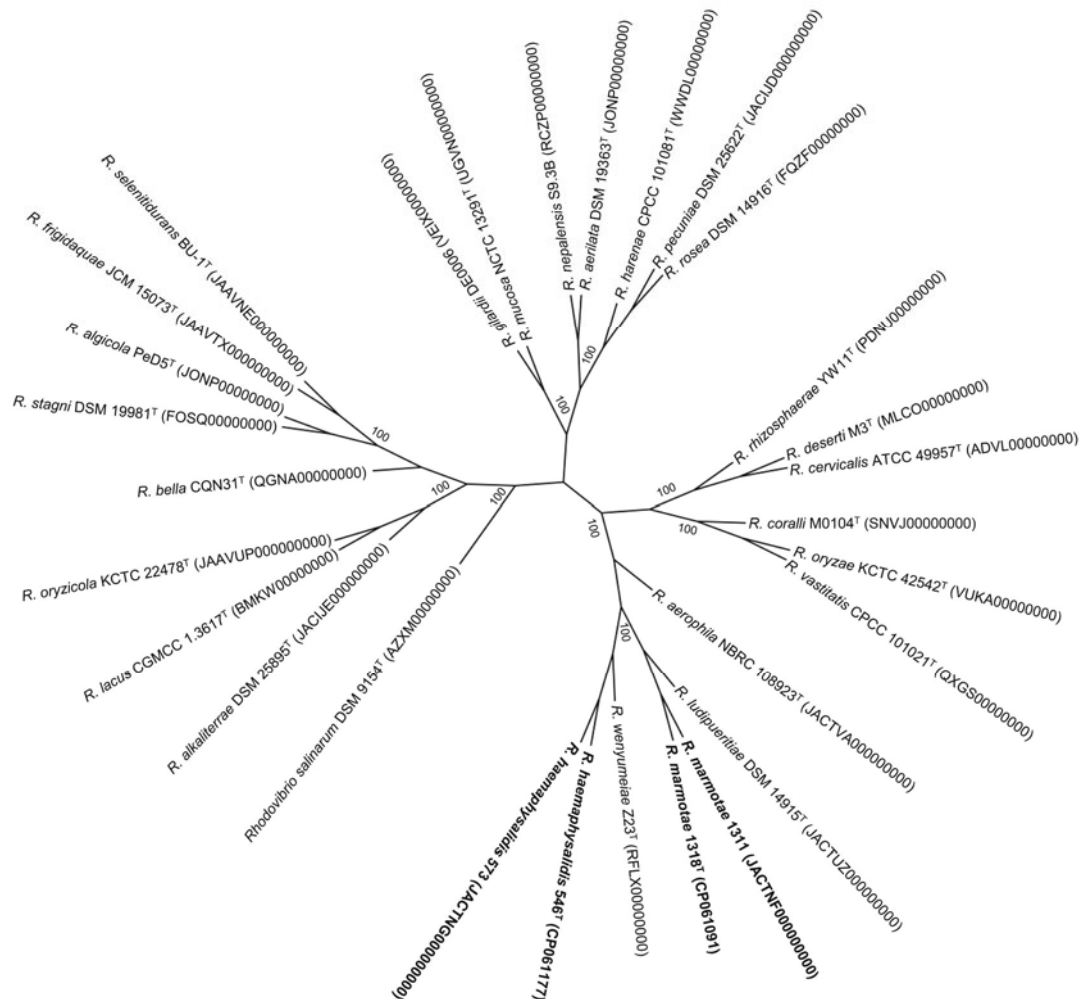
Fig. 2. Phylogenomic tree based on 238 core genes of the genus *Roseomonas*. Strains from this study are highlighted in bold. The outgroup is *Rhodovibrio salinarum* DSM 9154^T.

groups/pigments. One of the noticeable genetic differences between strains 546[T] and 1318[T] was that the former had 12 genes for iron acquisition and metabolism but none in the latter, suggesting that strain 546[T] had the advantage in an iron-deprived environment, e.g., tick's body (Brown *et al.*, 2002; Grosse *et al.*, 2006). Another remarkable difference was the flagellum gene operon in the chromosome of strain 546[T], which contrasted with strain 1318[T] in one of the plasmids p1318-2 (accession no. CP061093.1), which was consistent with zero genes in the chromosome of strain 1318[T] for motility and chemotaxis (Supplementary data Fig. S4B). Genes related to *β*-lactamase and resistance to fluoroquinolones were identified in both novel strains (with relatively detailed discussion in the *Antibiotic Resistance* part).

The prediction of potential secondary metabolites by antiSMASH from strains 546[T] and 1318[T] showed that the genome of strain 546[T] contained a gene cluster (position from 1,039,373 to 1,085,978) coding for carotenoid biosynthesis (conferring the colonies a distinct orange color), completely identical to that of *Enterobacteriaceae* bacterium DC404 (GenBank accession: DQ090834.1) and 70% similarity to that of *Brevundimonas vesicularis* (GenBank accession: DQ309446.1). Similarly, the genome of strain 1318[T] carried a gene cluster (position from 1,298,531 to 1,323,217) coding for (2R,3S,3'S)-2-hydroxyastaxanthin biosynthesis, with 83% similarity to that of *Paracoccus haeundaensis* (GenBank accession: AY-957386.1).

Phylogenomic analysis

Based on 0.5 protein identity, orthologous groups of 238 core genes shared by our isolates and all available genomes of the genus *Roseomonas* were extracted and used to build a phylogenomic tree (Fig. 2). This pangenomic tree revealed that strains 546[T], 573, 1318[T], and 1311 grouped with *R. wenyumeiae* Z23[T] and *R. ludipueritiae* DSM 14915[T], a result identical to that of phylogenetic trees based on 16S rRNA gene sequences.

Genomic relatedness and pangenome analysis

We next calculated genome-to-genome distances using ANI and digital DNA–DNA hybridization (dDDH). The dDDH scores within each strain pair were 99.9% (strains 546[T] and 573) and 99.7% (strains 1318[T] and 1311), well above the species threshold. In contrast, the scores of our isolates with their closest relatives were far below 70% (Richter and Rosselló-Móra, 2009), the cutoff for species demarcation (Fig. 3). The ANI values within each pair were 99.9%, in contrast to < 95% (Yoon *et al.*, 2017b) (Fig. 3) between our isolates and all established species of *Roseomonas*. These results suggested that strains 546[T], 573, 1318[T], and 1311 represented two novel species of the genus *Roseomonas*.

The differences in coding proteins when comparing genomes of *R. wenyumeiae* Z23[T], *R. ludipueritiae* DSM 14915[T], and strains 546[T], 573, 1318[T], and 1311 are shown in Fig. 4A. The genomes of strains 546[T] and 573 were most closely related

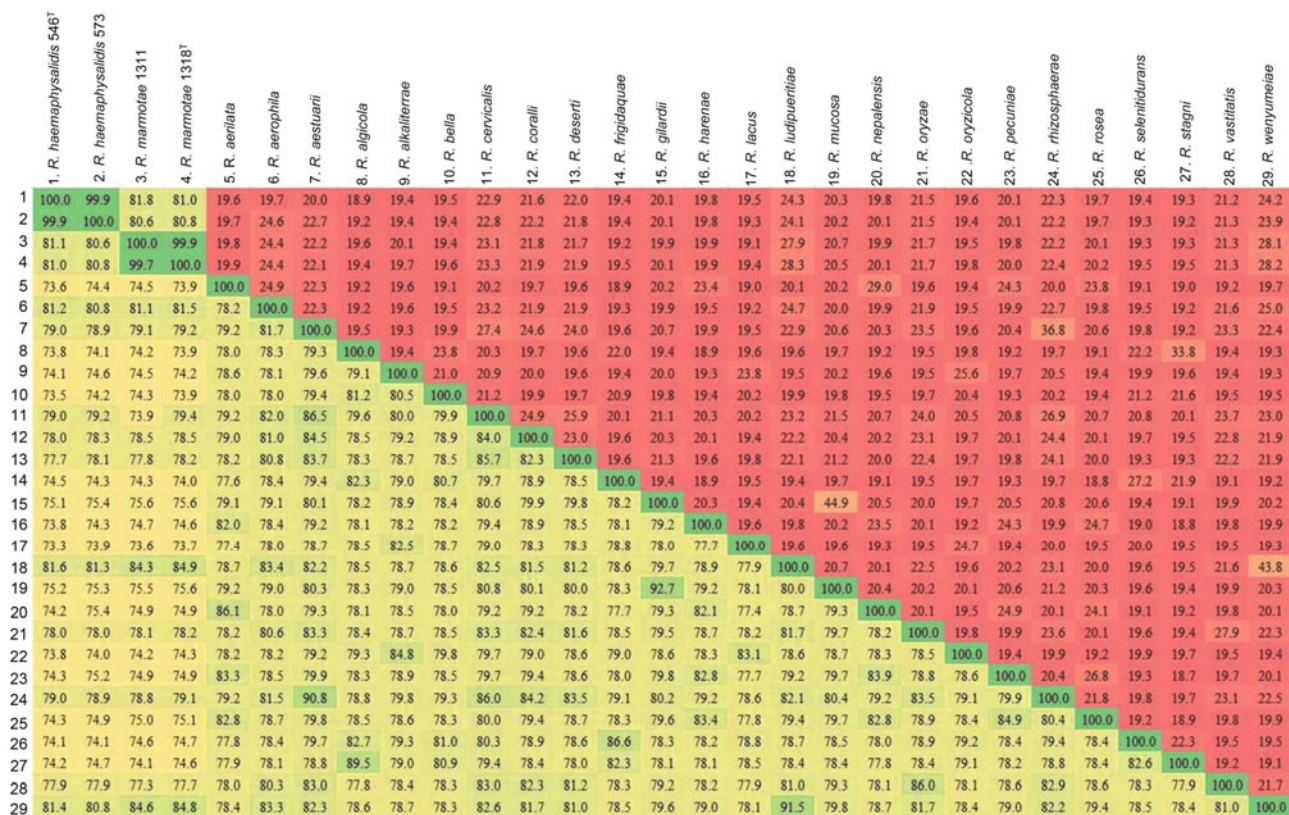|	1	2	3	4	5	6	7	8	9	10	11	12	13	14	15	16	17	18	19	20	21	22	23	24	25	26	27	28	29
1. R. haemaphysalidis 546T	100.0	99.9	81.8	81.0	19.6	19.7	20.0	18.9	19.4	19.5	22.9	21.6	22.0	19.4	20.1	19.8	19.5	24.3	20.3	19.8	21.5	19.6	20.1	22.3	19.7	19.4	19.3	21.2	24.2
2. R. haemaphysalidis 573	99.9	100.0	80.6	80.8	19.7	24.6	22.7	19.2	19.4	19.4	22.8	22.2	21.8	19.4	20.1	19.8	19.3	24.1	20.2	20.1	21.5	19.4	20.1	22.2	19.7	19.3	19.2	21.3	23.9
3. R. marmotae 1311	81.1	80.6	100.0	99.9	19.8	24.4	22.2	19.6	20.1	19.4	23.1	21.8	21.7	19.2	19.9	19.9	19.1	27.9	20.7	19.9	21.7	19.5	19.8	22.2	20.1	19.3	19.3	21.3	28.1
4. R. marmotae 1318T	81.0	80.8	99.7	100.0	19.9	24.4	22.1	19.4	19.7	19.6	23.3	21.9	21.9	19.5	20.1	19.9	19.4	28.3	20.5	20.1	21.7	19.8	20.0	22.4	20.2	19.5	19.5	21.3	28.2
5. R. aeriata	73.6	74.4	74.5	73.9	100.0	24.9	22.3	19.2	19.6	19.1	20.2	19.7	19.6	18.9	20.2	23.4	19.0	20.1	20.2	29.0	19.6	19.4	24.3	20.0	23.8	19.1	19.0	19.2	19.7
6. R. aerophila	81.2	80.8	81.1	81.5	78.2	100.0	22.3	19.6	19.5	19.5	23.2	21.9	21.9	19.3	19.9	19.5	19.2	24.7	20.0	19.9	21.9	19.5	19.9	22.7	19.8	19.5	19.2	21.6	25.0
7. R. aestuarii	79.0	78.9	79.1	79.2	79.2	81.7	100.0	19.5	19.3	19.3	27.4	24.6	24.0	19.6	20.7	19.9	19.5	22.9	20.6	20.3	23.5	19.6	20.4	36.8	20.6	19.8	19.2	22.3	22.4
8. R. algicola	73.8	74.1	74.2	73.9	78.0	78.3	79.3	100.0	19.4	23.8	20.3	19.7	19.6	22.0	19.4	18.9	19.6	19.6	19.7	19.2	19.5	19.8	19.2	19.7	19.1	22.2	33.8	19.4	19.3
9. R. alkaliterrae	74.1	74.6	74.5	74.2	78.6	78.1	79.6	79.1	100.0	21.0	20.9	20.0	19.6	19.4	20.0	19.3	23.8	19.5	20.2	19.6	19.5	25.6	19.7	20.5	19.4	19.9	19.6	19.4	19.3
10. R. bella	73.5	74.2	74.3	73.9	78.0	78.0	79.4	81.2	80.5	100.0	21.2	19.9	19.7	20.9	19.8	19.4	20.2	19.9	19.8	19.5	19.7	20.4	19.3	20.2	19.4	21.2	21.6	19.5	19.5
11. R. cervicalis	79.0	79.2	73.9	79.4	79.2	82.0	86.5	79.6	80.0	79.9	100.0	24.9	25.9	20.1	21.1	20.3	20.2	23.2	21.5	20.7	24.0	20.5	20.8	26.9	20.7	20.8	20.1	23.7	23.0
12. R. coralli	78.0	78.3	78.5	78.5	79.0	81.0	84.5	78.5	79.2	78.9	84.0	100.0	23.0	19.6	20.3	20.1	19.4	22.2	20.4	20.2	23.1	19.7	20.1	24.4	20.1	19.7	19.5	22.8	21.9
13. R. deserti	77.7	78.1	77.8	78.2	78.2	80.8	83.7	78.3	78.7	78.5	85.7	82.3	100.0	19.6	21.3	19.6	19.8	22.1	21.2	20.0	22.4	19.7	19.8	24.1	20.0	19.3	19.3	22.2	21.9
14. R. frigidaquae	74.5	74.3	74.3	74.0	77.6	78.4	79.4	82.3	79.0	80.7	79.7	78.9	78.5	100.0	19.4	18.9	19.5	19.4	19.7	19.1	19.5	19.7	19.3	19.7	18.8	27.2	21.9	19.1	19.2
15. R. gilardii	75.1	75.4	75.6	75.6	79.1	79.6	80.1	78.2	78.9	78.4	80.6	79.9	78.2	78.2	100.0	19.4	20.4	20.3	20.4	44.9	20.5	20.0	19.7	20.5	20.8	20.6	19.4	19.9	20.2
16. R. harenae	73.8	74.3	74.7	74.6	82.0	78.4	79.2	78.1	78.2	78.2	79.4	78.9	78.5	78.1	79.2	100.0	19.6	19.8	20.2	23.5	20.1	19.2	24.3	19.9	24.7	19.0	18.8	19.8	19.9
17. R. lacus	73.3	73.9	73.6	73.7	77.4	78.0	78.7	78.5	82.5	78.7	79.0	78.3	78.3	78.8	78.0	77.7	100.0	19.6	19.6	19.3	19.5	24.7	19.4	20.0	19.5	20.0	19.5	19.5	19.3
18. R. ludipueritiae	81.6	81.3	84.3	84.9	78.7	83.4	82.2	78.5	78.7	78.6	82.5	81.5	81.2	78.6	79.7	78.9	77.9	100.0	20.7	20.1	22.5	19.6	20.2	23.1	20.0	19.6	19.5	21.6	43.8
19. R. mucosa	75.2	75.3	75.5	75.6	79.2	79.0	80.3	78.3	79.0	78.5	80.8	80.1	80.0	78.3	92.7	79.2	78.1	80.0	100.0	20.4	20.2	20.1	20.6	21.2	20.3	19.6	19.4	19.9	20.3
20. R. nepalensis	74.2	75.4	74.9	74.9	86.1	78.0	79.3	78.1	78.5	78.0	79.2	79.2	78.2	77.7	79.3	82.1	77.4	78.7	79.3	100.0	20.1	19.5	24.9	20.1	24.1	19.1	19.2	19.8	20.1
21. R. oryzae	78.0	78.0	78.1	78.2	78.2	80.6	83.3	78.4	78.7	78.5	83.3	82.4	81.6	78.5	79.5	78.7	78.2	81.7	79.7	78.2	100.0	19.8	19.9	23.6	20.1	19.6	19.4	27.9	22.3
22. R. oryzicola	73.8	74.0	74.2	74.3	78.2	78.2	79.2	79.3	84.8	79.8	79.7	79.0	78.6	79.0	78.6	78.3	83.1	78.6	78.7	78.3	78.5	100.0	19.4	19.9	19.2	19.9	19.7	19.5	19.4
23. R. pecuniae	74.3	75.2	74.9	74.9	83.3	78.5	79.9	78.3	79.6	78.5	79.7	79.4	78.6	78.0	79.8	82.8	77.7	79.2	79.7	82.8	78.6	78.6	100.0	20.4	26.8	19.3	18.7	19.7	20.1
24. R. rhizosphaerae	79.0	78.9	78.8	79.1	79.2	81.5	90.8	78.8	79.8	79.3	86.0	84.2	83.5	79.1	80.2	79.2	78.6	82.1	80.4	79.2	83.5	79.1	79.9	100.0	21.8	19.8	19.7	23.1	22.5
25. R. rosea	74.3	74.9	75.0	75.1	82.8	78.7	79.8	78.5	78.6	78.3	80.0	79.4	78.7	79.6	83.4	77.8	79.4	79.7	82.8	78.4	84.9	80.4	79.4	79.9	100.0	19.2	18.9	19.8	19.9
26. R. seleniidurans	74.1	74.1	74.6	74.7	77.8	78.4	79.7	82.7	79.3	81.0	80.3	78.9	78.6	86.6	78.3	78.2	78.8	78.7	78.5	78.0	78.9	79.2	78.4	79.4	78.4	100.0	22.3	19.5	19.5
27. R. stagni	74.2	74.7	74.1	74.6	77.9	78.1	78.8	89.5	79.0	80.9	79.4	78.4	78.0	82.3	78.1	78.1	78.5	78.4	78.4	77.8	78.4	79.1	78.2	78.8	78.4	82.6	100.0	19.2	19.1
28. R. vastitatis	77.9	77.9	77.3	77.7	78.0	80.3	83.0	77.8	78.4	78.3	83.0	82.3	81.2	78.3	79.2	78.2	77.9	81.0	79.3	78.1	86.0	78.1	78.6	82.9	78.6	78.3	77.9	100.0	21.7
29. R. wenyumeiae	81.4	80.8	84.6	84.8	78.4	83.3	82.3	78.6	78.7	78.3	82.6	81.7	81.0	78.5	79.6	79.0	78.1	91.5	79.8	78.7	81.7	79.4	79.0	82.2	79.4	78.5	78.4	81.0	100.0

Fig. 3. Heat map showing ANI (lower diagonal) and dDDH (upper diagonal) values between our isolates and the members of the genus *Roseomonas*.
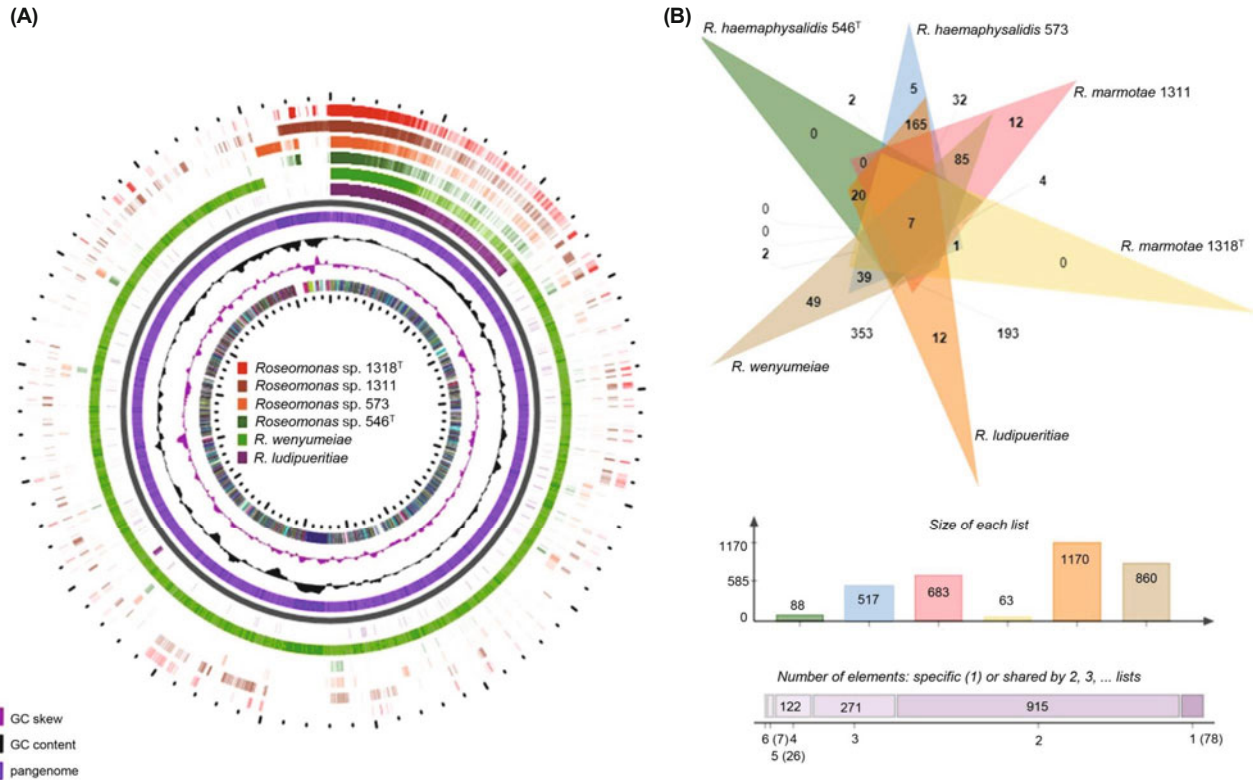
(A)

(B)

Fig. 4. Comparative analysis among the genomes of *R. wenyumeiae* Z23[T], *R. ludipueritiae* DSM 14915[T], and strains 546[T], 573, 1318[T], and 1311. (A) Pangenome analysis. The inner-most slot (purple) shows the constructed pangenome. (B) Venn diagram showing the number of shared and unique orthologous genes.

to those of strains 1318[T] and 1311. Pangenome analysis of these four newly obtained genomes represented by Venn diagrams (Fig. 4B) illustrated that together with the two genomes of their closest relatives, there were 1,419 orthologous clusters, containing seven core clusters (GO accession numbers: 0030288, 0005886, 0009236, 0055072, 0006189, 0019284, and 0006814) and including 140 proteins.

Antibiotic resistance and pathogenicity

Antibiotic resistance was evaluated using the E-test and demonstrated that strains 546[T], 573, 1318[T], and 1311 were resistant to four types of antibiotics, aminoglycosides (amikacin and gentamicin), tetracyclines, β-lactams (cefepime, ceftriaxone, meropenem, and oxacillin), and quinolones (ciprofloxacin), a pattern distinct from *R. wenyumeiae* Z23[T], which was sensitive to gentamicin and ciprofloxacin (Tian *et al.*, 2019). In addition, strains 546[T] and 573 were moderately resistant to chloramphenicol. A part of our results is consistent with a previous report showing that *Roseomonas* species are highly resistant to β-lactams (Ioannou *et al.*, 2020). An antimicrobial resistance (AMR) gene family was found in strains 546[T] (3,180 bp) and 1318[T] (3,168 bp) using the Comprehensive Antibiotic Resistance Database, which showed 82% nucleotide similarity with each other and 90.0% and 91.2% amino acid identity to that of *R. pecuniae*, respectively. It also revealed a gene encoding the multidrug (quinolone and tetracycline) efflux RND transporter permease subunit.

Roseomonas species can cause opportunistic infections in immunocompromised individuals. The genomes of tick-derived strains 546[T] and 573 contained several virulence genes that encoded lipopolysaccharide (LPS), flagella, capsule, hemolysin, urease, type III secretion system (T3SS), and type IV secretion system (T4SS) effectors. They could be participating in bacterial pathogenicity, such as adhesion, hemolysis, resistance, and transportation of virulence factors (Tosi *et al.*, 2013; Pechstein *et al.*, 2020). Further studies should pay more attention to this aspect.

Chemotaxonomic properties

$C_{18:1}\omega7c$ and $C_{16:1}\omega7c/C_{16:1}\omega6c$ were the two major fatty acids shared by all four isolates with $C_{16:0}$ predominant in strains 546[T] and 573, and $C_{19:0}$ cyclo $\omega8c$ in strains 1311 and 1318[T] (Table 3). Compared to their three closest neighbors (excluding *R. aerophila* NBRC 108923[T]), strains 546[T] and 573 had more $C_{16:0}$ and $C_{18:1}\omega7c$ but less $C_{19:0}$ cyclo $\omega8c$ and/or even none of $C_{14:0}$ 2-OH. Strains 1311 and 1318[T] had more $C_{16:1}\omega7c/C_{16:1}\omega6c$ than all other strains as shown in Table 3. In addition, the rare fatty acid $C_{18:1}$ 2-OH was detected in four novel strains and three reference strains with varying content (Table 3). The respiratory quinone analyses revealed that strains 546[T] and 1318[T] shared the same set of quinones, with an almost equal amount of Q-10 (91.4% *vs.* 93.3%), Q-9 (6.0% *vs.* 4.8%) and Q-8 (2.6% *vs.* 2.0%), more or less similar to *R. aerophila* NBRC 108923[T] and *R. ludipueritiae* DSM 14915[T] with predominant Q-10 and others unspecified (Kämpfer *et al.*, 2003; Kim *et al.*, 2013). However, these were different

Table 3. Cellular fatty acid contents (> 1%) of our isolates and the closely related type strains of the genus *Roseomonas*
Strains: 1, *Roseomonas haemaphysalidis* 546[T]; 2, *Roseomonas haemaphysalidis* 573; 3, *Roseomonas marmotae* 1311; 4, *Roseomonas marmotae* 1318[T]; 5, *R. wenyumeiae* Z23[T]; 6, *R. ludipueritiae* DSM 14915[T]; 7, *R. aerophila* NBRC 108923[T]. –, less than 1%. All data are from this study.

Strains	1	2	3	4	5	6	7
$C_{14:0}$	1.2	1.4	1.9	2.1	4.5	2.9	1.1
$C_{14:0}$ 2-OH	–	–	5.9	5.7	4.5	5.6	–
$C_{16:1}\omega7c/C_{16:1}\omega6c$	15.5	16.5	22.4	22.1	18.0	7.7	8.2
$C_{16:1}\omega5c$	3.4	3.2	6.6	5.9	8.3	4.6	3.5
$C_{16:0}$	17.6	17.7	6.5	7.4	7.8	11.4	10.6
$C_{16:0}$ 3-OH	2.5	–	2.0	1.8	1.8	–	1.1
$C_{17:0}$ cyclo	–	1.4	2.4	2.8	2.2	–	–
$C_{18:1}\omega7c$	43.7	44.2	33.9	32.9	29.7	36.7	52.7
$C_{17:0}$ iso 3-OH	1.9	–	2.5	–	4.7	3.2	2.5
$C_{19:0}$ cyclo $\omega8c$	3.1	3.2	11.0	12.6	10.6	10.6	8.2
$C_{18:1}$ 2-OH	7.0	7.6	2.5	2.1	2.0	13.0	5.9

from *R. wenyumeiae* Z23[T] with 100% of Q-10 (Tian *et al.*, 2019). Analyses of polyamine pattern revealed that all four strains contained spermidine as the major component, which is the common trait in the genus *Roseomonas* (Tian *et al.*, 2019).

Although certain unidentified phospholipids and lipids in strains 546[T] and 1318[T] were not exactly at the same position (Supplementary data Fig. S5), their polar lipid profiles shared diphosphatidylglycerol (DPG), phosphatidylethanolamine (PE), phosphatidylglycerol (PG), and phosphatidylcholine (PC) with their closest relatives. In comparison, the two novel type strains lacked aminolipid (*vs.* all others) and amino-phospholipid (*vs. R. wenyumeiae* Z23[T]) but had more/less unidentified phospholipids (5 *vs.* 2 in *R. wenyumeiae* Z23[T] and none in the other two) and lipids (2 *vs.* 10 in *R. ludipueritiae* DSM 14915[T] and none in *R. aerophila* NBRC 108923[T]).

Taxonomic conclusion

Altogether, the aforementioned biochemical, chemotaxonomic, phenotypic, phylogenetic, and phylogenomic differences provide sufficient evidence to distinguish our four isolates from their closely related type strains. These results reveal them as two novel species of the genus *Roseomonas*. With 546[T] and 1318[T] as the type strains, we suggest the names *Roseomonas haemaphysalidis* sp. nov. and *Roseomonas marmotae* sp. nov. for the two novel members of the genus *Roseomonas*.

Description of *Roseomonas haemaphysalidis* sp. nov.

Roseomonas haemaphysalidis (hae.ma.phy.sa'li.dis. N.L. gen. n. *haemaphysalidis*, of a tick of the genus *Haemaphysalis*).

The cells are Gram-negative, non-spore forming, catalase- and oxidase-positive, mesophilic, motile, and cocci-shaped with sizes between 1.5 and 1.9 μm. The colonies are orange, circular, and smooth with sizes between 1.0 and 1.3 mm after 3 days of growth. They can produce acid from D-arabinose, L-arabinose, D-fructose, D-fucose, L-fucose, D-lyxose, D-ribose, and D-xylose, but not from glycerol, erythritol, D-adonitol, D-galactose, D-glucose, D-mannose, L-sorbose, dulcitol, inositol, D-mannitol, D-sorbitol, amygdalin, arbutin, esculin, D-maltose, D-lactose, glycogen, D-arabitol, or L-arabitol. Enzymatic activities are positive for esterase (C4), esterase lipase (C8), leucine arylamidase, α-glucosidase, but negative for lipase (C14), valine arylamidase, cysteine arylamidase, trypsine arylamidase, α-galactosidase, β-galactosidase, β-glucu-

ronidase, β-glucosidase, α-fucosidase, and α-mannosidase. They are positive for urea hydrolysis. $C_{18:1}\omega7c$, $C_{16:1}\omega7c/C_{16:1}\omega6c$, and $C_{16:0}$ are the predominant fatty acids, DPG and PE are the major polar lipids, and Q-10 is the primary respiratory quinone. The major polyamine is spermidine.

The type strain 546[T] (= GDMCC 1.1780[T] = JCM 34187[T]), isolated from *Haemaphysalis longicornis* collected from Jiangxi Province of China, has a DNA G + C content of 70.9%. Strain 573 is also classified in this species. The GenBank/EMBL/DDBJ accession numbers of strains 546[T] and 573 are MW-405824 and MW405823 (16S rRNA gene), and CP061177 and JACTNG000000000 (genome), respectively.

Description of *Roseomonas marmotae* sp. nov.

Roseomonas marmotae (mar.mo'tae. N.L. fem. n. *marmotae*, referring to strain isolation from *Marmota himalayana*).

The cells are Gram-negative, catalase- and oxidase-positive, non-spore forming, mesophilic, motile, and cocci-shaped with sizes between 1.7 and 2.1 μm. The colonies are white, circular, and smooth with sizes between 0.7 and 0.9 mm after 3 days of growth. They can produce acid from D-arabinose, L-arabinose, D-fucose, and L-fucose, D-lyxose, D-melibiose, L-rhamnose, D-ribose, D-xylose, L-xylose, and D-fructose (variable), but not from glycerol, erythritol, D-adonitol, D-galactose, D-glucose, D-mannose, L-sorbose, dulcitol, inositol, D-mannitol, D-sorbitol, amygdalin, arbutin, esculin, D-maltose, D-lactose, glycogen, D-arabitol, or L-arabitol. In addition, enzymatic activities are positive for esterase (C4) and leucine arylamidase, but negative for lipase (C14), valine arylamidase, cysteine arylamidase, trypsine arylamidase, α-galactosidase, β-galactosidase, β-glucuronidase, β-glucosidase, α-fucosidase, and α-mannosidase. Nitrate reduction is positive. $C_{18:1}\omega7c$, $C_{16:1}\omega7c/C_{16:1}\omega6c$, and $C_{19:0}$ cyclo $\omega8c$ are the predominant fatty acids, DPG and PE are the major polar lipids, and Q-10 is the primary respiratory quinone. The major polyamine is spermidine.

The type strain 1318[T] (= GDMCC 1.1781[T] = JCM 34188[T]), isolated from the respiratory tract of marmot collected from the Qinghai Tibet plateau of China, has a DNA G + C content of 69.2%. Strain 1311 is also classified in this species. The GenBank/EMBL/DDBJ accession numbers of strains 1318[T] and 1311 are MW410945 and MW410944 (16S rRNA gene), and CP061091 and JACTNF000000000 (genome), respectively.

Acknowledgements

Conflict of Interest

The authors declare that they have no conflict of interest.

References

Alcock, B.P., Raphenya, A.R., Lau, T.T.Y., Tsang, K.K., Bouchard, M., Edalatmand, A., Huynh, W., Nguyen, A.L.V., Cheng, A.A., Liu, S., *et al.* 2020. CARD 2020: antibiotic resistome surveillance with the comprehensive antibiotic resistance database. *Nucleic Acids Res.* **48**, D517–D525.

Athalye, M., Noble, W.C., and Minnikin, D.E. 1985. Analysis of cellular fatty acids by gas chromatography as a tool in the identification of medically important coryneform bacteria. *J. Appl. Bacteriol.* **58**, 507–512.

Aziz, R.K., Bartels, D., Best, A.A., DeJongh, M., Disz, T., Edwards, R.A., Formsma, K., Gerdes, S., Glass, E.M., Kubal, M., *et al.* 2008. The RAST server: rapid annotations using subsystems technology. *BMC Genomics* **9**, 75.

Blin, K., Shaw, S., Steinke, K., Villebro, R., Ziemert, N., Lee, S.Y., Medema, M.H., and Weber, T. 2019. antiSMASH 5.0: updates to the secondary metabolite genome mining pipeline. *Nucleic Acids Res.* **47**, W81–W87.

Booth, J.K., Page, J.E., and Bohlmann, J. 2017. Terpene synthases from *Cannabis sativa*. *PLoS ONE* **12**, e0173911.

Brown, J.S., Gilliland, S.M., Ruiz-Albert, J., and Holden, D.W. 2002. Characterization of pit, a *Streptococcus pneumoniae* iron uptake ABC transporter. *Infect. Immun.* **70**, 4389–4398.

Chin, C.S., Alexander, D.H., Marks, P., Klammer, A.A., Drake, J., Heiner, C., Clum, A., Copeland, A., Huddleston, J., Eichler, E.E., *et al.* 2013. Nonhybrid, finished microbial genome assemblies from long-read SMRT sequencing data. *Nat. Methods* **10**, 563–569.

Collins, M.D. and Jones, D. 1981. Distribution of isoprenoid quinone structural types in bacteria and their taxonomic implication. *Microbiol. Rev.* **45**, 316–354.

Dantas-Torres, F., Chomel, B.B., and Otranto, D. 2012. Ticks and tick-borne diseases: a One Health perspective. *Trends Parasitol.* **28**, 437–446.

Dé, I., Rolston, K.V.I., and Han, X.Y. 2004. Clinical significance of *Roseomonas* species isolated from catheter and blood samples: analysis of 36 cases in patients with cancer. *Clin. Infect. Dis.* **38**, 1579–1584.

Frank, J.A., Reich, C.I., Sharma, S., Weisbaum, J.S., Wilson, B.A., and Olsen, G.J. 2008. Critical evaluation of two primers commonly used for amplification of bacterial 16S rRNA genes. *Appl. Environ. Microbiol.* **74**, 2461–2470.

Fu, L., Niu, B., Zhu, Z., Wu, S., and Li, W. 2012. CD-HIT: accelerated for clustering the next-generation sequencing data. *Bioinformatics* **28**, 3150–3152.

Grosse, C., Scherer, J., Koch, D., Otto, M., Taudte, N., and Grass, G. 2006. A new ferrous iron-uptake transporter, EfeU (YcdN), from *Escherichia coli*. *Mol. Microbiol.* **62**, 120–131.

Guerrero, F.D., Miller, R.J., and Pérez de León, A.A. 2012. Cattle tick vaccines: many candidate antigens, but will a commercially viable product emerge? *Int. J. Parasitol.* **42**, 421–427.

Ioannou, P., Mavrikaki, V., and Kofteridis, D.P. 2020. *Roseomonas* species infections in humans: a systematic review. *J. Chemother.* **32**, 226–236.

Jain, C., Rodriguez-R, L.M., Phillippy, A.M., Konstantinidis, K.T., and Aluru, S. 2018. High throughput ANI analysis of 90K prokaryotic genomes reveals clear species boundaries. *Nat. Commun.* **9**, 5114.

Kämpfer, P., Andersson, M.A., Jäckel, U., and Salkinoja-Salonen, M. 2003. *Teichococcus ludipueritiae* gen. nov. sp. nov., and *Muricoccus roseus* gen. nov. sp. nov. representing two new genera of the α-1 subclass of the *Proteobacteria*. *Syst. Appl. Microbiol.* **26**, 23–29.

Kim, K.R., Kim, K.H., Khan, S.A., Kim, H.M., Han, D.M., and Jeon, C.O. 2021. *Lysobacter arenosi* sp. nov. and *Lysobacter solisilvae* sp. nov. isolated from soil. *J. Microbiol.* **59**, 709–717.

Kim, S.J., Weon, H.Y., Ahn, J.H., Hong, S.B., Seok, S.J., Whang, K.S., and Kwon, S.W. 2013. *Roseomonas aerophila* sp. nov., isolated from air. *Int. J. Syst. Evol. Microbiol.* **63**, 2334–2337.

Kumar, S., Stecher, G., Li, M., Knyaz, C., and Tamura, K. 2018. MEGA X: molecular evolutionary genetics analysis across computing platforms. *Mol. Biol. Evol.* **35**, 1547–1549.

Lee, D.C., Kang, H., Weerawongwiwat, V., Kim, B., Choi, Y.W., and Kim, W. 2013. *Oceanobacillus chungangensis* sp. nov., isolated from a sand dune. *Int. J. Syst. Evol. Microbiol.* **63**, 3666–3671.

Li, F., Huang, Y., Hu, W., Li, Z., Wang, Q., Huang, S., Jiang, F., and Pan, X. 2021. *Roseomonas coralli* sp. nov., a heavy metal resistant bacterium isolated from coral. *Int. J. Syst. Evol. Microbiol.* **71**. doi: 10.1099/ijsem.0.004624.

Liu, Y., Du, J., Zhang, J., Lai, Q., Shao, Z., and Zhu, H. 2020. *Parahaliea maris* sp. nov., isolated from surface seawater and emended description of the genus *Parahaliea*. *J. Microbiol.* **58**, 92–98.

Mulita, F., Oikonomou, N., Provatidis, A., Alexopoulos, A., and Maroulis, I. 2020. *Roseomonas gilardii* in patient with leukemia and acute appendicitis: case report and review. *Pan Afr. Med. J.* **36**, 283.

Oh, Y.J., Kim, J.Y., Jo, H.E., Park, H.K., Lim, S.K., Kwon, M.S., and Choi, H.J. 2020. *Lentibacillus cibarius* sp. nov., isolated from kimchi, a Korean fermented food. *J. Microbiol.* **58**, 387–394.

Pechstein, J., Schulze-Luehrmann, J., Bisle, S., Cantet, F., Beare, P.A., Ölke, M., Bonazzi, M., Berens, C., and Lührmann, A. 2020. The *Coxiella burnetii* T4SS effector AnkF is important for intracellular replication. *Front. Cell. Infect. Microbiol.* **10**, 559915.

Price, M.N., Dehal, P.S., and Arkin, A.P. 2009. FastTree: computing large minimum evolution trees with profiles instead of a distance matrix. *Mol. Biol. Evol.* **26**, 1641–1650.

Richter, M. and Rosselló-Móra, R. 2009. Shifting the genomic gold standard for the prokaryotic species definition. *Proc. Natl. Acad. Sci. USA* **106**, 19126–19131.

Rihs, J.D., Brenner, D.J., Weaver, R.E., Steigerwalt, A.G., Hollis, D.G., and Yu, V.L. 1993. *Roseomonas*, a new genus associated with bacteremia and other human infections. *J. Clin. Microbiol.* **31**, 3275–3283.

Rossi-Tamisier, M., Benamar, S., Raoult, D., and Fournier, P.E. 2015. Cautionary tale of using 16S rRNA gene sequence similarity values in identification of human-associated bacterial species. *Int. J. Syst. Evol. Microbiol.* **65**, 1929–1934.

Sánchez-Porro, C., Gallego, V., Busse, H.J., Kämpfer, P., and Ventosa, A. 2009. Transfer of *Teichococcus ludipueritiae* and *Muricoccus roseus* to the genus *Roseomonas*, as *Roseomonas ludipueritiae* comb. nov. and *Roseomonas rosea* comb. nov., respectively, and emended description of the genus *Roseomonas*. *Int. J. Syst. Evol. Microbiol.* **59**, 1193–1198.

Shao, S., Guo, X., Guo, P., Cui, Y., and Chen, Y. 2019. *Roseomonas mucosa* infective endocarditis in patient with systemic lupus erythematosus: case report and review of literature. *BMC Infect. Dis.* **19**, 140.

Tao, C.Q., Ding, Y., Zhao, Y.J., and Cui, H.L. 2020. *Natronorubrum*

halophilum sp. nov. isolated from two inland salt lakes. *J. Microbiol.* **58**, 105–112.

Tian, Z., Lu, S., Jin, D., Yang, J., Pu, J., Lai, X.H., Wang, X.X., Wu, X.M., Li, J., Wang, S., *et al.* 2019. *Roseomonas wenyumeiae* sp. nov., isolated from faeces of Tibetan antelopes (*Pantholops hodgsonii*) on the Qinghai-Tibet Plateau. *Int. J. Syst. Evol. Microbiol.* **69**, 2979–2986.

Tosi, T., Pflug, A., Discola, K.F., Neves, D., and Dessen, A. 2013. Structural basis of eukaryotic cell targeting by type III secretion system (T3SS) effectors. *Res. Microbiol.* **164**, 605–619.

Venkata Ramana, V., Sasikala, C., Takaichi, S., and Ramana, C.V. 2010. *Roseomonas aestuarii* sp. nov., a bacteriochlorophyll-a containing alphaproteobacterium isolated from an estuarine habitat of India. *Syst. Appl. Microbiol.* **33**, 198–203.

Watanabe, M., Aoyagi, Y., Ohta, A., and Minnikin, D.E. 1997. Structures of phenolic glycolipids from *Mycobacterium kansasii*. *Eur. J. Biochem.* **248**, 93–98.

Yokoyama, A., Miki, W., Izumida, H., and Shizuri, Y. 1996. New trihydroxy-keto-carotenoids isolated from an astaxanthin-producing marine bacterium. *Biosci. Biotechnol. Biochem.* **60**, 200–203.

Yoon, S.H., Ha, S.M., Kwon, S., Lim, J., Kim, Y., Seo, H., and Chun, J. 2017a. Introducing EzBioCloud: a taxonomically united database of 16S rRNA gene sequences and whole-genome assemblies. *Int. J. Syst. Evol. Microbiol.* **67**, 1613–1617.

Yoon, S.H., Ha, S.M., Lim, J., Kwon, S., and Chun, J. 2017b. A large-scale evaluation of algorithms to calculate average nucleotide identity. *Antonie van Leeuwenhoek* **110**, 1281–1286.

Zerbino, D.R. and Birney, E. 2008. Velvet: algorithms for *de novo* short read assembly using de Bruijn graphs. *Genome Res.* **18**, 821–829.

Zhu, W., Yang, J., Lu, S., Lai, X.H., Jin, D., Pu, J., Wang, X., Huang, Y., Zhang, S., Huang, Y., *et al.* 2019. *Fudania jinshanensis* gen. nov., sp. nov., isolated from faeces of the Tibetan antelope (*Pantholops hodgsonii*) in China. *Int. J. Syst. Evol. Microbiol.* **69**, 2942–2947.

Zhu, W., Yang, J., Lu, S., Lai, X.H., Jin, D., Wang, X., Pu, J., Ren, Z., Huang, Y., Wu, X., *et al.* 2020. *Actinomyces qiguomingii* sp. nov., isolated from the *Pantholops hodgsonii*. *Int. J. Syst. Evol. Microbiol.* **70**, 58–64.

Zhu, W., Yang, J., Lu, S., Lan, R., Jin, D., Luo, X.L., Pu, J., Wu, S., and Xu, J. 2021. Beta- and novel delta-coronaviruses are identified from wild animals in the Qinghai-Tibetan plateau, China. *Virol. Sin.* **36**, 402–411.